A Hierarchical Control Strategy for Underwater Vehicle

Teng Zhang [a], Shoudong Huang [a], Dikai Liu [a]

[a] *Centre for Autonomous Systems, University of Technology, Sydney, Ultimo, NSW 2007, Australia*

Abstract

In this paper, the problem of trajectory tracking in 3D space for a fully actuated autonomous underwater vehicle (AUV) is addressed and a novel hierarchical control scheme is proposed. In this scheme, the kinematics of AUV and the highly uncertain dynamics of AUV are treated separately where the kinematics are formulated on the Special Euclidean group $SE(3)$. On the kinematic level, a bounded and smooth virtual velocity is designed. The vehicle will follow the desired trajectory if the vehicle's velocity converges to the virtual velocity. On the dynamic level, two model-free controllers for virtual velocity tracking are developed. The hierarchical design avoids the orientation singularity, and simplifies the complexity of the trajectory tracking problem such that many existing methods for the control of uncertain nonlinear systems can be used. Moreover, the bounded and smooth design of the virtual velocity is helpful to reduce the amplitude of the control input.

Key words: autonomous underwater vehicle; hierarchical control scheme; trajectory tracking.

1 Introduction

In the past few decades, the related sensor fusion techniques have significantly improved the navigation capability of AUVs. A typical task for an underwater vehicle navigation is to design a robust controller such that the underwater vehicle accurately follows a desired trajectory. The problem of trajectory tracking is now reasonably well understood for a holonomic system in Euclidean space. However, it is not the case for an AUV because vehicle dynamics in the underwater environment are highly uncertain. For this reason, various advanced control strategies for AUVs have been proposed and can be roughly classified as two categories: model-based control and model-free control.

Model-based control for an AUV employs a finite-dimensional lumped parameter dynamic model to describe the hydrodynamics of the AUV. Some controllers are available based on the nominal model with exact parameters, such as [1] and [2]. However, there is not a commonly accepted method to calculate the parameters in the nominal dynamic model for vehicles. In [3–7], several experiment-based methods for parameter identification are introduced and these usually require expensive devices, such as a towing tank, with dedicated instrumentation and manoeuvres. In recent years, parameter identification for AUV by computational fluid dynamics (CFD) software is reported in [8] and [9]. On the other hand, trajectory tracking control for a class of fully actuated nonlinear systems (i.e., $\dot{x} = f(x)\Theta + u$ where $f(x)$ is a known nonlinear function and Θ are unknown constants) is well studied in [10] and the related theoretical results are utilized by many model-based adaptive controllers, such as [11–15]. A common point of these model-based adaptive controllers is designing a filter to identify the unknown parameters online. A similar idea by identifying parameters in the nominal model online is reported in [16] and [17] in which sliding mode control and optimal control are used, respectively. An obvious drawback for model-based control is that it is difficult to handle the large unmodeled error and the time-varing external disturbance. It is reported in [15] and [18] that without additional supplementary techniques some model-based controllers may not guarantee stability in the presence of unmodeled error such as the thruster dynamics during highly dynamic vehicle maneuvering.

Unlike model-based control, model-free control for AUVs does not explicitly depend on a nominal dynamic model. Hence its adaptability seems more flexible compared to model-based control from the most intuitive point of view. The unknown hydrodynamic effects can be treated as an uncertain nonlinear function. Based on this viewpoint, the popular techniques such as neural networks-based and fuzzy logic control are used to approximate the hydrodynamic effects in model-free control of AUVs, e.g., [19–21]. In [22] and [23], a nonlinear controller is reported in which a disturbance observer is designed to adapt to the unknown dynamics. In [24], a continuous Robust Integral of the Sign of

Email addresses: Teng.Zhang@uts.edu.au (Teng Zhang), Shoudong.Huang@uts.edu.au (Shoudong Huang), Dikai.Liu@uts.edu.au (Dikai Liu).

the Error (RISE) control structure is proposed for a class of multiple-input multiple-output (MIMO) nonlinear systems and a RISE type controller for AUVs is developed in [25], requiring some prior knowledge of the upper bounds of the uncertain vehicle dynamics for the control gain selection.

Besides the uncertain dynamics, another issue for AUV control is that the problem is formulated in non-Euclidean space because vehicle's orientation in 3D space is a point in the special orthogonal group $SO(3)$. For addressing the orientation in 3D space, ZYX Euler-angle (roll, pitch and yaw) as a local parameterization of $SO(3)$ is widely employed. Therefore the problem in non-Euclidean space can be formulated in Euclidean space. Recently, the exponential coordinate is used to represent vehicle's orientation in [15]. However, singularities, at which rotational rate matrix is undefined, can never be eliminated in any 3-dimensional representation of $SO(3)$ including the exponential coordinates and ZYX Euler-angle [26]. Therefore, the controllers using Euler-angle or exponential coordinate does not always work well when the vehicle singularity happens. Fewer controllers for AUVs employ unit quaternion as orientation representation. In [13], a model-based controller with unit quaternion as orientation representation is proposed but it is difficult to directly use unit quaternion for most Euler-angle based model-free controllers. For example, the controllers proposed in [20], [23] and [27] strongly depend on the assumption that the vehicle's orientation is always far away from the singularity orientation. Therefore, additional supplemental techniques should be used when the vehicle is close to a singularity orientation.

To address the difficulties mentioned above, a hierarchical control scheme is proposed in this paper. The scheme consists of the kinematics level and the dynamics level. Firstly, a 6-dimensional vector called "virtual velocity" is desinged on the kinematic level according to the vehicle's pose, the desired trajectory and the desired velocity. The vehicle' pose will follow the desired trajectory if the vehicle's velocity converges to the virtual velocity. Secondly, the dynamics level generates the control input signals such that the vehicle's velocity converges to the virtual velocity.

The contributions of this paper are in four aspects:

- The hierarchical design simplifies the complexity of the trajectory tracking problem, because the kinematics and the dynamics are treated separately. The proposed virtual velocity provides a solution for the kinematic level such that the rest of the trajectory tracking problem is designing a controller for the "virtual velocity" tracking on the dynamic level.
- Many existing methods for the control of the uncertain nonlinear systems can be used on the dynamic level after some minor modifications. In this paper, two model-free controllers for "virtual velocity" tracking are developed. Hierarchical design has high potential of being coupled with the more advanced controller in the future.
- The virtual linear velocity is deliberately designed to be bounded and smooth, which is shown to be very helpful to reduce the amplitude of the inputs especially when the vehicle is far away from the desired trajectory.
- The problem of orientation singularity is skillfully avoided by the design of virtual velocity on the kinematic level. Thus this control scheme can handle the situation where the pitch angle is near 90° without any additional supplemental techniques.

This paper is organized as follows. In Section 2, the kinematic and dynamic model of an AUV is described and the trajectory tracking problem is formulated. In Section 3, the virtual velocity is designed with detailed step descriptions. In Section 4, based on the available methods in the literature, two model-free controllers for virtual velocity tracking are proposed with stability analysis. In Section 5, our designed control scheme is illustrated and validated through a number of comparisons between the original controllers and the modified controllers. Section 6 states conclusion and future work.

2 Problem Formulation

The motion of an underwater vehicle can be modeled as the motion of a rigid body. Let O be an inertial coordinate frame. Let B be a coordinate frame fixed in the vehicle and coincides with the center of mass of the underwater vehicle. The coordinate transformation from the frame B to the frame O can be expressed by $g = (R, p) \in SE(3)$, e.g., for a point q in 3D space, $q|_O = Rq|_B + p$ where $q|_O$ denotes the coordinate of q in the frame O and $q|_B$ denotes the coordinate of q in the frame B. The matrix $R \in SO(3)$ denotes the rotation from the frame B to the frame O. The vector $p \in \mathbb{R}^3$ is the coordinate of the origin of the frame B, expressed in the frame O. Because the frame B is fixed relative to the vehicle, the vehicle's pose can also be represented by g. Let $V := (v^T, \omega^T)^T \in \mathbb{R}^6$ be the general velocity of the frame B relative to the frame O, where $v \in \mathbb{R}^3$ is the linear velocity of the frame B relative to the frame O, expressed in the frame B and $\omega \in \mathbb{R}^3$ is the angular velocity of the frame B relative to the frame O, expressed in the frame B.

The kinematic equation of the underwater vehicle can be expressed as:

$$\begin{aligned} \dot{R} &= Rs(\omega) \\ \dot{p} &= Rv \end{aligned} \tag{1}$$

where the linear operator s is the skew symmetric operator, defined as

$$s(x) = \begin{pmatrix} 0 & -x_3 & x_2 \\ x_3 & 0 & -x_1 \\ -x_2 & x_1 & 0 \end{pmatrix}, \ \forall x = (x_1, x_2, x_3)^T \in \mathbb{R}^3. \tag{2}$$

According to [11] and [28], the dynamic equation of AUV can be described as

$$M\dot{V} + C(V)V + D(V)V + \mathscr{G} + d = u, \tag{3}$$

where $M \in \mathbb{R}^{6\times6}$ denotes the inertial matrix including added mass, $C(V) \in \mathbb{R}^{6\times6}$ denotes the centripetal terms and the Coriolis matrix, $D(V) \in \mathbb{R}^{6\times6}$ denotes the damping matrix describing the effect of drag force, $\mathscr{G}$ denotes the restoring force produced by the gravity and the buoyancy, $d \in \mathbb{R}^6$ denotes the unmodeled error including the external disturbances and $u \in \mathbb{R}^6$ as the control input denotes the force and torque expressed in the frame B produced by thrusters or other actuators. The problem considered in this paper can be stated as follows.

Trajectory tracking for a fully actuated underwater vehicle: Let $g_d(t) = (R_d(t), p_d(t)) : 0 \leq t < \infty$ be a desired trajectory in the group $SE(3)$ and assumed to be bounded and smooth with respect to t and its first-order derivative and second-order derivative are bounded. The problem is to design a controller $u \in \mathbb{R}^6$ such that the vehicle's pose $g(t)$ converges to the desired trajectory $g_d(t)$. It is assumed that the vehicle's pose g and velocity V are always available.

3 Kinematic Level

In this section a virtual velocity V_r is designed such that if the vehicle's velocity V converges to the virtual velocity V_r, the vehicle's pose g will converge to the desired trajectory g_d.

Firstly, a "distance" function $\mathbf{V}_1(g, g_d)$ on $SE(3)$ is defined:

$$\mathbf{V}_1(g, g_d) = \frac{1}{2}\Delta\theta^2 + \frac{1}{2}\|p - p_d\|^2 \tag{4}$$

where $\Delta\theta = \arccos(\frac{tr(RR_d^T)-1}{2}) \in [0, \pi]$ represents the rotation angle of the rotation matrix RR_d^T [26], R_d is the desired orientation and p_d is the desired position. The time derivative of $\Delta\theta$ is

$$\begin{aligned}\Delta\dot{\theta} &= \frac{1}{\sqrt{1-(\frac{tr(RR_d^T)-1}{2})^2}}\frac{tr(\dot{R}R_d^T + R\dot{R}_d^T)}{2} \\ &= \frac{1}{sin\Delta\theta}\frac{tr(Rs(\omega-\omega_d)R_d^T)}{2} \\ &= \frac{1}{sin\Delta\theta}\frac{tr(R_d^T Rs(\omega-\omega_d))}{2}\end{aligned} \tag{5}$$

where ω_d is the desired angular velocity derived from (1) and the desired trajectory g_d. Notice that $tr(\bar{R}s(w)) = -(\bar{R} - \bar{R}^T)^{\curlyvee T}w$ for any $\bar{R} \in SO(3)$ and any $w \in \mathbb{R}^3$, where the operator $\curlyvee$ is a mapping from 3×3 skew symmetric matrix to 3-dimensional vector, defined as

$$\begin{pmatrix} 0 & -a_3 & a_2 \\ a_3 & 0 & -a_1 \\ -a_2 & a_1 & 0 \end{pmatrix}^{\curlyvee} = \begin{pmatrix} a_1 \\ a_2 \\ a_3 \end{pmatrix} \tag{6}$$

And hence (5) can be rewritten as

$$\Delta\dot{\theta} = \frac{-1}{2sin\Delta\theta}(R_d^T R - (R_d^T R)^T)^{\curlyvee T}(\omega - \omega_d) \tag{7}$$

Note that $R_d^T R - (R_d^T R)^T = 2sin\Delta\bar{\theta}s(W)$ where $\Delta\bar{\theta}$ is the rotation angle of $R_d^T R$ and W is the rotation axis of $R_d^T R$ defined as

$$W = \frac{1}{2\|R_d^T R - (R_d^T R)^T\|}(R_d^T R - (R_d^T R)^T)^{\curlyvee} \tag{8}$$

On the other hand,

$$\Delta\theta = \arccos(\frac{tr(RR_d^T)-1}{2}) = \arccos(\frac{tr(R_d^T R)-1}{2}) = \Delta\bar{\theta} \tag{9}$$

and hence (7) can be rewritten as

$$\Delta\dot{\theta} = -W^T(\omega - \omega_d) \tag{10}$$

By combining (4) with (10), the time derivative of $\mathbf{V}_1(g, g_d)$ can be written as

$$\begin{aligned}\dot{\mathbf{V}}_1 &= -\Delta\theta W^T(\omega-\omega_d) + (p-p_d)^T(\dot{p}-\dot{p_d}) \\ &= -\Delta\theta W^T(\omega-\omega_d) + (p-p_d)^T(Rv - R_d v_d)\end{aligned} \tag{11}$$

where v_d is the desired linear velocity derived from (1) and the desired trajectory g_d. For analyzing $\dot{\mathbf{V}}_1$, a virtual velocity $V_r = (v_r^T, \omega_r^T)^T$ is designed as

$$v_r = R^T R_d v_d - k_1 R^T \frac{p-p_d}{\|p-p_d\|}(1 - e^{-\|p-p_d\|}) \tag{12}$$

$$\omega_r = \frac{2k_2}{\sqrt{1+\cos\Delta\theta}}(R_d^T R - (R_d^T R)^T)^{\curlyvee} + \omega_d \tag{13}$$

where k_1 and k_2 are positive control gains. By combining (11) with (12) and (13), $\dot{\mathbf{V}}_1$ can be rewritten as

$$\begin{aligned}\dot{\mathbf{V}}_1 = &-4k_2\frac{\sin\Delta\theta}{\sqrt{1+\cos\Delta\theta}}\Delta\theta - k_1\|p-p_d\|(1-e^{-\|p-p_d\|}) \\ &- W^T\Delta\theta(\omega-\omega_r) + (p-p_d)(Rv - Rv_r)\end{aligned} \tag{14}$$

In the following paragraph, we prove that if $V \to V_r$, i.e., $v \to v_r$ and $\omega \to \omega_r$ then $\mathbf{V}_1 \to 0$, i.e., $g \to g_d$. If $V \to V_r$, then $\forall\ \varepsilon \in (0, k_2)$, $\exists\ T_\varepsilon$, $\|v - v_r\| < \varepsilon$ and $\|\omega - \omega_r\| < \varepsilon$ for $t \geq T_\varepsilon$. On the other hand,

$$4\frac{\sin\Delta\theta}{\sqrt{1+\cos\Delta\theta}} \geq \Delta\theta, \tag{15}$$

when $\Delta\theta \in [0, \pi)$. Then $\forall\ t \geq T_\varepsilon$

$$\dot{\mathbf{V}}_1 \leq -k_2\Delta\theta^2 + \varepsilon\Delta\theta - \|p-p_d\|(k_1 - k_1 e^{-\|p-p_d\|} - \varepsilon) \tag{16}$$

and hence it is obvious that $\dot{\mathbf{V}}_1 < 0$ if $\Delta\theta > \frac{\varepsilon}{k_2}$ and $\|p - p_d\| > \ln\frac{k_1}{k_1-\varepsilon}$ when $t > T_\varepsilon$. On the other hand, $\mathbf{V}_1$ increases with respect to $\Delta\theta$ and $\|p-p_d\|$, respectively. Therefore,

$$\limsup_{t\to\infty} \mathbf{V}_1 \leq \mathbf{V}_1|_{\Delta\theta=\frac{\varepsilon}{k_2},\|p-p_d\|=\ln\frac{k_1}{k_1-\varepsilon}} \leq (\frac{1}{k_1^2}+\frac{1}{2k_2^2})\varepsilon^2, \tag{17}$$

when ε is small enough. According to the arbitrariness of ε, it is concluded that

$$\limsup_{t\to\infty} \mathbf{V}_1 = 0, \tag{18}$$

i.e., $\mathbf{V}_1 \to 0$ and hence $g \to g_d$. The next subsection will consider how to design a controller such that $V \to V_r$.

Remark 1: Note that the formulation of (12): the term $\frac{p-p_d}{\|p-p_d\|}(1-e^{-\|p-p_d\|}) \approx \frac{p-p_d}{\|p-p_d\|}$ when $\|p-p_d\|$ is large and $\frac{p-p_d}{\|p-p_d\|}(1-e^{-\|p-p_d\|}) \approx p-p_d$ when $\|p-p_d\|$ is small and hence v_r is bounded and smooth if the desired linear velocity v_d is bounded and smooth. On the other hand, ω_r is well defined and bounded if ω_d is bounded because $\Delta\theta \in [0,\pi]$ and

$$\frac{\|(R_d^T R-(R_d^T R)^T)^\vee\|}{\sqrt{1+\cos\Delta\theta}} = \frac{2\sin\Delta\theta}{\sqrt{1+\cos\Delta\theta}} \to 2\sqrt{2}, \Delta\theta \to \pi^- \tag{19}$$

In all, this design of (12) and (13) make the virtual velocity V_r bounded and smooth. In Section 5, it is demonstrated through simulation that the design is helpful to reduce the amplitude of the control input signals on the dynamic level.

4 Dynamic Level

In this section, we address the problem of designing a controller for the uncertain nonlinear system expressed in (3) such that $V \to V_r$. Two model-free controllers (Controller 1+ and Controller 2+) based on the existing methods in [23] and [27] are developed to validate the proposed hierarchical control scheme.

4.1 Model-free Controller 1+

In [29], a model-free controller is reported that forces the actual velocity to track the desired velocity. In [23], the extended controller based on Euler-angle for trajectory-tracking is proposed. In the following, based on the work in [29], the improved Controller 1+ is proposed that requires weaker assumptions: $\|M^{-1}\| \leq \alpha$, $\|M\| \leq \beta_1$, $\lambda_{min}(M^{-1}) > r$, $\|C(V)+D(V)\| \leq \beta_2+\beta_3\|e\|$, and $\|\mathscr{G}+d\| \leq d_0+d_1\|e\|$, where $\lambda_{min}(M^{-1})$ represents the smallest eigenvalue of M^{-1} and $e := V_r - V$. Let $\theta_1 = \frac{\alpha\beta_1}{r}$, $\theta_2 = \frac{\alpha\beta_2}{r}$, $\theta_3 = \frac{\alpha d_0}{r}$, $\theta_4 = \frac{\varepsilon+\alpha d_1}{r}$, $\theta_5 = \frac{\alpha\beta_3}{r}$ where ε is a positive constant and hence θ_i $(i = 1,...,5)$ is a positive constant.

The proposed controller is designed as

$$u = \sum_{i=1}^{5} K_i\phi_i, \tag{20}$$

where $\phi_1 = \dot{V}_r$, $\phi_2 = V$, $\phi_3 = 1$, $\phi_4 = e$ and $\phi_5 = \|e\|\|V\|(1,0,0,0,0,0)^T$. The update law for K_i is

$$K_i = \frac{\hat{\theta}_i e\phi_i^T}{\|e\|\|\phi_i\|}, \tag{21}$$

$$\dot{\hat{\theta}}_i = f_i\|e\|\|\phi_i\| \tag{22}$$

where f_i $(i = 1,...,5)$ is a positive control gain and the initial value $\hat{\theta}_i(0)$ $(i = 1,...,5)$ is designed to be nonnegative.

Then the following is the proof that e converges to zero. A Lyapunov function is defined as

$$\mathbf{V}_2 = \frac{1}{2}e^T e + \frac{1}{2}\sum_{i=1}^{5} f_i^{-1} r(\theta_i - \hat{\theta}_i)^2 \tag{23}$$

With (3) and (20), the time derivative of $\mathbf{V}_2$ becomes

$$\begin{aligned}\dot{\mathbf{V}}_2 =& [e^T M^{-1}\sum_{i=1}^{5} P_i\phi_i - \sum_{i=1}^{5} f_i^{-1} r\theta_i\dot{\hat{\theta}}_i] \\ &+ [-e^T M^{-1}\sum_{i=1}^{5} K_i\phi_i + \sum_{i=1}^{5} f_i^{-1} r\hat{\theta}_i\dot{\hat{\theta}}_i]\end{aligned} \tag{24}$$

where $P_1 = M$, $P_2 = C(V)+D(V)$, $P_3 = \mathscr{G}+d$, $P_4 = 0$ and $P_5 = 0$.

With the update law (21) and (22), the formula in the first bracket of (24) can be derived as

$$\begin{aligned}&e^T M^{-1}\sum_{i=1}^{5} P_i\phi_i - \sum_{i=1}^{5} f_i^{-1} r\theta_i\dot{\hat{\theta}}_i \\ &= e^T M^{-1}\sum_{i=1}^{2} P_i\phi_i + e^T M^{-1}P_3\phi_3 - \sum_{i=1}^{5} r\theta_i\|e\|\|\phi_i\| \\ &= (e^T M^{-1}\sum_{i=1}^{2} P_i\phi_i - \sum_{i=1}^{2}\alpha\beta_i\|e\|\|\phi_i\|) + e^T M^{-1}(\mathscr{G}+d) \\ &\quad - \alpha d_0\|e\|\|\phi_3\| - (\varepsilon+\alpha d_1)\|e\|\|\phi_4\| - \alpha\beta_3\|e\|\|\phi_5\| \\ &\leq \|e\|\alpha(\beta_1\|\phi_1\| + \beta_2\|\phi_2\| + \beta_3\|e\|\|\phi_2\|) \\ &\quad - \sum_{i=1}^{2}\alpha\beta_i\|e\|\|\phi_i\| + \|e\|\alpha(d_0 + d_1\|e\|) \\ &\quad - \alpha d_0\|e\| - (\varepsilon+\alpha d_1)\|e\|^2 - \alpha\beta_3\|e\|\|\phi_5\| \\ &\leq -\varepsilon\|e\|^2 + \alpha\beta_3\|V\|\|e\|^2 - \alpha\beta_3\|e\|\|e\|\|V\| \\ &\leq -\varepsilon\|e\|^2\end{aligned} \tag{25}$$

and the formula in the second bracket can be derived as

$$\begin{aligned}
&-e^T M^{-1}\sum_{i=1}^{5} K_i\phi_i + \sum_{i=1}^{5} f_i^{-1} r\hat{\theta}_i\dot{\hat{\theta}}_i \\
&= -e^T M^{-1}\sum_{i=1}^{5}\frac{\hat{\theta}_i e\phi_i^T}{\|e\|\|\phi_i\|}\phi_i + \sum_{i=1}^{5} f_i^{-1} r\hat{\theta}_i f_i\|e\|\|\phi_i\| \\
&= \sum_{i=1}^{5}\frac{-e^T M^{-1} e}{\|e\|}\|\phi_i\|\hat{\theta}_i + \sum_{i=1}^{5} r\hat{\theta}_i\|e\|\|\phi_i\| \\
&\leq \sum_{i=1}^{5}(-\lambda_{min}(M^{-1}) + r)\|e\|\|\phi_i\|\hat{\theta}_i
\end{aligned} \tag{26}$$

From (25) and (26), it is clear that $\dot{\mathbf{V}}_2 < 0$ when $e \neq 0$ and hence $e \to 0$, i.e., $V \to V_r$.

Remark 2: Large control input signals and high-frequency oscillation would be generated by the proposed controller shown in (21). In order to alleviate this problem, a modified version is used:

$$K_i = \begin{cases} \frac{\hat{\theta}_i e\phi_i^T}{\|e\|\|\phi_i\|} & \text{if } \|e\|\|\phi_i\| > \delta_i \\ \frac{\hat{\theta}_i e\phi_i^T}{\delta_i} & \text{if } \|e\|\|\phi_i\| \leq \delta_i \end{cases} \tag{27}$$

In order to avoid ambiguities, Controller 1+ refers to (20), (22) and (27) with the virtual velocity (12) and (13). Controller 1 refers to the controller in [23]. Compared to Controller 1+, Controller 1 requires the assumption $\|C(V) + D(V)\| \leq \beta_2$, while a weaker assumption $\|C(V) + D(V)\| \leq \beta_2 + \beta_3\|e\|$ is required in our proposed Controller 1+.

4.2 Model-free Controller 2+

An Euler-angle based controller reported in [27] successfully applies the RISE type feedback in [24] to an AUV, which requires the knowledge of the upper bounds of the overall system uncertainty. Here we propose an improved controller (such that $V \to V_r$) based on the recent RISE type control structure in [30], which requires the assumptions: $\dot{M}$, V_r and $\dot{V}_r$ are bounded, $0 < M_{min} \leq \|M\| \leq M_{max}$ and the term $C(V)V + D(V)V + \mathscr{G} + d$ is uniformly continuous with respect to time t and continuously differentiable up to its second-order derivatives. The proposed controller is

$$u = k(e - e(0)) + \int_0^t ke\,\mathrm{d}\tau + \int_0^t \beta Sgn(e)\,\mathrm{d}\tau \tag{28}$$

where $k > 1$ is a control gain to be selected, $e = V_r - V \in \mathbb{R}^6$, $Sgn(e) = (sgn(e_1), ...sgn(e_6))^T \in \mathbb{R}^6$, and $\beta \in \mathbb{R}$ is updated according to

$$\beta = \beta_0 + e^T Sgn(e) - e(0)^T Sgn(e(0)) + \int_0^t e^T Sgn(e)\,\mathrm{d}\tau \tag{29}$$

where $\beta_0 > 1$ is a constant to be chosen.

The following provides a simplified proof for the stability of the controller above. Firstly, the standard hydrodynamic equation (3) can be rewritten as

$$M\dot{V} + f = u \tag{30}$$

where M is the unknown inertia matrix including added mass and $f = C(V)V + D(V)V + \mathscr{G} + d$ is also unknown. Two auxiliary variables $\mathbf{r} \in \mathbb{R}^6$ and $z \in \mathbb{R}^{12}$ are defined as

$$\mathbf{r} = \dot{e} + e \tag{31}$$

and

$$z = (e^T, \mathbf{r}^T)^T \tag{32}$$

By combining (30) with (29) and (31), $\dot{\beta}$ can be obtained:

$$\dot{\beta} = \mathbf{r}^T Sgn(e) \tag{33}$$

By combining (30) with (31), $\dot{\mathbf{r}}$ can be obtained:

$$M\dot{\mathbf{r}} = -\frac{1}{2}\dot{M}\mathbf{r} - e - \dot{u} + N \tag{34}$$

where

$$N = M(\ddot{V}_r + \dot{e}) + \dot{M}(\frac{1}{2}\mathbf{r} + \dot{V}) + \dot{f} + e \tag{35}$$

The term N consists of two parts, i.e., $N = N_r + \bar{N}$, where $N_r = N|_{V=V_r, \dot{V}=\dot{V}_r}$ and $\bar{N} = N - N_r$. Note that N_r and $\dot{N}_r$ are bounded because M, $\dot{M}$, V_r and $\dot{V}_r$ are bounded, i.e., $\forall\ t$, $\exists\ K > 0$ such that $\max_{1\leq i\leq 6}|N_{ri}| \leq K$, $\max_{1\leq i\leq 6}|\dot{N}_{ri}| \leq K$. Moreover, according to the Mean Value Theorem [31], $\bar{N}$ can be bounded such that

$$\|\bar{N}\| \leq p(\|z\|)\|z\| \tag{36}$$

where $p : \mathbb{R}_{\geq}0 \to \mathbb{R}_{\geq}0$ is a globally invertible, non-decreasing function.

Lemma 1 ([24]): A function $L_1(t) \in \mathbb{R}$ is defined as

$$L_1 = \mathbf{r}^T(N_r - 2KSgn(e)). \tag{37}$$

According to the property of K: $K \geq \|N_r\|, \|\dot{N}_r\|$, we have

$$\int_0^t L_1(\tau)\,\mathrm{d}\tau \leq \eta_1, \tag{38}$$

where η_1 is a positive constant.

Lemma 2 ([30]): A function $L_2(t) \in \mathbb{R}$ is defined as

$$L_2 = -\dot{e}^T Sgn(e) \tag{39}$$

Then we have

$$\int_0^t L_2(\tau)\,\mathrm{d}\tau \leq \eta_2 \tag{40}$$

where η_2 is a positive constant.

Then three variables are defined as

$$P_1 = \eta_1 - \int_0^t L_1(\tau)\,\mathrm{d}\tau > 0 \tag{41}$$

$$P_2 = \beta_0(\eta_2 - \int_0^t L_2(\tau)\,\mathrm{d}\tau) > 0 \tag{42}$$

$$P_3 = \beta - \beta_0 - 2K \tag{43}$$

A Lyapunov function $\mathbf{V}_3$ respect to $y := (z^T, \sqrt{P_1}, \sqrt{P_2}, P_3)^T$ is defined as

$$\mathbf{V}_3 = \frac{1}{2}e^T e + \frac{1}{2}\mathbf{r}^T M\mathbf{r} + \frac{1}{2}P_3^2 + P_1 + P_2 \tag{44}$$

After taking the time derivative of (44), $\dot{\mathbf{V}}_3$ can be obtained:

$$\begin{aligned}
\dot{\mathbf{V}}_3 &= e^T\dot{e} + (\mathbf{r}^T M\dot{\mathbf{r}} + \frac{1}{2}\mathbf{r}^T\dot{M}\mathbf{r}) \\
&\quad + (\beta - \beta_0 - 2K)\mathbf{r}^T Sgn(e) - L_1 - \beta_0 L_2 \\
&= -e^T e - k\mathbf{r}^T\mathbf{r} + \mathbf{r}^T\bar{N} - \beta_0 e^T Sgn(e) \\
&= -e^T e - \mathbf{r}^T\mathbf{r} - (k-1)\mathbf{r}^T\mathbf{r} + \mathbf{r}^T\bar{N} - \beta_0 e^T Sgn(e) \\
&\le -\|z\|^2 - ((k-1)\|\mathbf{r}\|^2 - \|\mathbf{r}\|p(\|z\|)\|z\|) - \beta_0 e^T Sgn(e) \\
&\le -\|z\|^2 + \frac{p^2(\|z\|)}{4(k-1)}\|z\|^2 - \beta_0 e^T Sgn(e)
\end{aligned} \tag{45}$$

From the inequality, $\dot{\mathbf{V}}_3 < 0$ when $e \neq 0$ and $\|y\| \le p^{-1}(\sqrt{4(k-1)})$. On the other hand, note that $0 < M_{min} \le \|M\| \le M_{max}$ which implies $a_1\|y\|^2 \le \mathbf{V}_3 \le a_2\|y\|^2$, where $a_1 = min\{\frac{1}{2}, M_{min}\}$ and $a_2 = max\{2, M_{max}\}$. By using Theorem 8.4 in [31], it is followed that $\mathbf{V}_3 \to 0$ when $\|y(0)\|$ is less than a value related to k, i.e., k is selected larger than a value related to $\|y(0)\|$, which implies $g \to g_d$.

Remark 3: In order to avoid ambiguities, Controller 2+ refers to (28) and (29) with the virtual velocity (12) and (13). Controller 2 refers to the controller in [27]. Note that in Controller 2, β is a constant based on the prior knowledge while β is time-varying in the proposed Controller 2+ and hence Controller 2+ relies less on prior knowledge of the uncertain system.

5 Simulation Results

A performance comparison between the proposed controllers and their original controllers has been made by numerical simulations. The dynamic model of the ODIN vehicle is used in the simulation. This model has been validated through experiments, e.g., [32] and [33].

5.1 Settings

In order to show effectiveness of the proposed hierarchical control scheme, Control 1+ is compared with Controller 1 in Section 5.2, and Controller 2+ is compared with Controller 2+ in Section 5.3. The rotation angle $\Delta\theta$, the generalized position error $\|p - p_d\| \in \mathbb{R}^+$ and the input $u \in \mathbb{R}^6$ are used in the comparisons, where $\Delta\theta$ is the rotation angle between the desired orientation and the actual orientation, given as

$$\Delta\theta = \arccos(\frac{tr(RR_d^T) - 1}{2}) \in [0, \pi]. \tag{46}$$

In all simulations, the vehicle's initial state is set as

$$\begin{aligned}
R_0 &= I_3, & p_0 &= (5,0,0)^T \\
v_0 &= (0,0,0)^T, & \omega_0 &= (0,0,0)^T
\end{aligned} \tag{47}$$

Two desired trajectories are used to illustrate the behavior of the controllers. The first desired trajectory is

$$\begin{aligned}
R_d(t) &= R_z(-t/10) \\
p_d(t) &= (2\sin(t/10), 2\cos(t/10), t/20)^T
\end{aligned} \tag{48}$$

and the second trajectory is

$$\begin{aligned}
R_d(t) &= R_y(-t/10) \\
p_d(t) &= (0,0,t/20)^T
\end{aligned} \tag{49}$$

where R_z denotes the rotation about z-axis and R_y denotes the rotation about y-axis. The second trajectory is designed such that the singularity happens when $t = (2n+1)5\pi$ where $n \in \mathbb{Z}^+$. At the beginning, the vehicle's position is far away from the desired trajectory. In the simulation, the parameters of Controller 1 are chosen as: $\sigma = 1$, $\hat{\theta}_i = 0$, $f_i = 1$, $\delta_i = 0.1$ $(i = 1, ..., 5)$. In oder to achieve similar tracking performance, the parameters of Controller 1+ are chosen as: $k_1 = 4$, $k_2 = \sqrt{2}$, $\hat{\theta}_i = 0$, $f_i = 1$ and $\delta_i = 0.1$ $(i = 1, .., 5)$. The parameters for Controller 2 are $\alpha_i = 1$ $(i = 1, 2)$, $k_s = 200$ and $\beta = 20$. In oder to achieve similar tracking performance, the parameters for Controller 2+ are chosen as: $k_1 = 1$, $k_2 = \frac{\sqrt{2}}{2}$, $k = 200$ and $\beta_0 = 20$.

5.2 Controller 1 vs Controller 1+

5.2.1 The first desired trajectory

For the first desired trajectory, both Controller 1 and Controller 1+ can stabilize the simulated vehicle after 25s. Fig. 1 displays the generalized position error of Controller 1 and Controller 1+ during $0 \sim 25s$. Fig. 2 displays the rotation angle between the desired orientation and the actual orientation of Controller 1 and Controller 1+ during $0 \sim 25s$. Table 1 displays the maximal amplitudes of the inputs by Controller 1 and Controller 1+ during $0 \sim 25s$. Table 2 displays

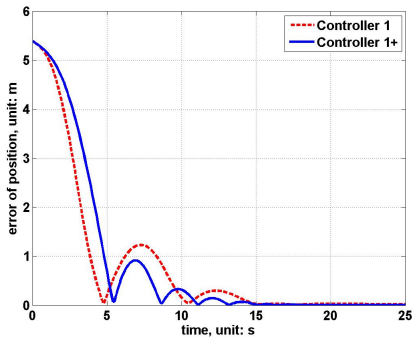

Fig. 1. The simulated generalized position error for the first desired trajectory during $0 \sim 25s$: Controller 1 and Controller 1+

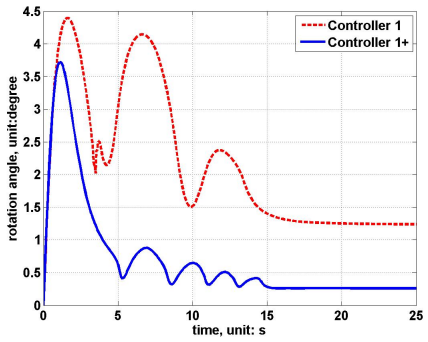

Fig. 2. The simulated rotation angle for the first desired trajectory during $0 \sim 25s$: Controller 1 and Controller 1+

the average amplitudes of the inputs by Controller 1 and Controller 1+ during $0 \sim 25s$.

As shown in Fig. 1, Controller 1 has slightly better performance in the position tracking than Controller 1+ before 5s however a slightly poorer performance than Controller 1+ after 5s. From Fig. 2, we can see that Controller 1+ has much better performance in the rotation tracking than Controller 1: the convergence rate is faster and the final error is smaller. It is shown in Table 1 that the maximal amplitudes of all inputs by Controller 1+ are much smaller than that by Controller 1, especially for u_6. It is shown in Table 2 that the average amplitudes of all inputs (except u_3) by Controller 1+ are smaller than that by Controller 1, and the average amplitude of u_6 by Controller 1+ is a little bigger than that by Controller 1. In this simulation, u_4 and u_5 generated by both controllers are very small (less than 0.0005) and therefore 0 is listed in Table 1 and Table 2. In Fig. A.1 and A.2 in Appendix, the control inputs u_1 and u_6 under the two controllers are displayed to show the large differences.

5.2.2 *The second desired trajectory*

For the second desired trajectory, it is shown in Fig. 3 that the simulated vehicle is stabilized by the proposed Controller 1+. In this simulation, Controller 1 suddenly generates huge control input signals and it forces the vehicle to

Table 1
The maximal amplitudes (max.am) of inputs by Controller 1 and Controller 1 for the first desired trajectory during $0 \sim 25s$

Ctr/max.am	u_1	u_2	u_3	u_4	u_5	u_6
Ctr 1	190	85.8	20.0	0	0	121.6
Ctr 1+	103.4	39.9	6.8	0	0	5.57

Table 2
The average amplitudes (ave.am) of inputs by Controller 1 and Controller 1 for the first desired trajectory during $0 \sim 25s$

Ctr/ave.am	u_1	u_2	u_3	u_4	u_5	u_6
Ctr 1	36.9	13.5	1.73	0	0	4.67
Ctr 1+	20.38	9.7	1.91	0	0	2.32

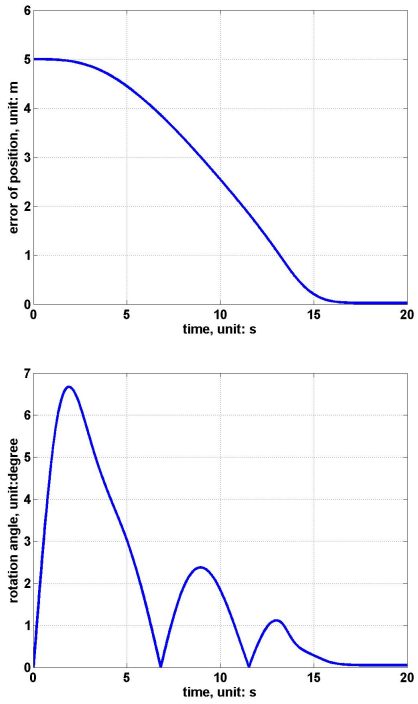

Fig. 3. The simulated generalized position error and rotation angle for the second desired trajectory during $0 \sim 20s$: Controller 1+

an unreasonable position when the pitch angle is close to $-90°$, which results in the failure of tracking. Controller 1 requires the pitch angle always far away from $90°$, however this is not the case for the second desired trajectory.

5.3 *Controller 2 vs Controller 2+*

5.3.1 *The first desired trajectory*

It is shown in Fig. 4 and Fig. 5 that the simulated vehicle can track the first desired trajectory under both Controller 2 and Controller 2+. As we can see from Fig. 4, Controller 2 achieves better performance in the position tracking than Controller 2+ before 10s and a very slightly poorer performance than Controller 2+ after 10s. Fig. 5 shows that Con-

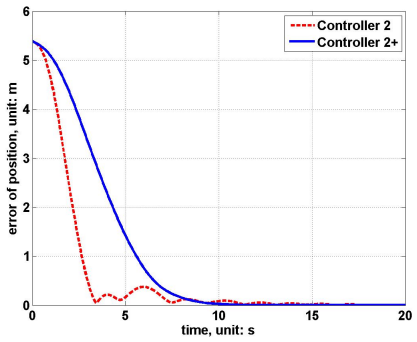

Fig. 4. The simulated generalized position error for the first desired trajectory: Controller 2 and Controller 2+

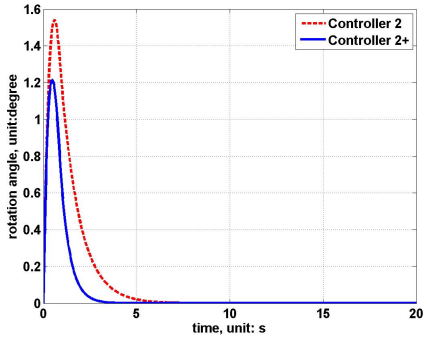

Fig. 5. The simulated rotation angle for the first desired trajectory: Controller 2 and Controller 2+

troller 2+ performs better than Controller 2 for the rotation tracking due to the faster convergence rate and the smaller final error. It is shown in Table 3 that the maximal amplitudes of u_1 and u_2 by Controller 2+ are much smaller than that by Controller 2 in this simulation. Table 4 shows that Controller 2+ generates smaller control inputs signals, especially for u_1 and u_2 in this simulation. In Fig. A.3 and A.4 in Appendix, the control inputs u_1 and u_2 are displayed to show the large difference in amplitudes of the two controllers.

Table 3
The maximal amplitudes (max.am) of inputs by Controller 2 and Controller 2+ during $0 \sim 20s$ for the first desired trajectory

Ctr/max.am	u_1	u_2	u_3	u_4	u_5	u_6
Ctr 2	406	152	19.03	0.016	0.018	5.44
Ctr 2+	91.67	37.18	16.27	0.015	0.009	5.51

Table 4
The average amplitudes (ave.am) of inputs by Controller 2 and Controller 2+ during $0 \sim 20s$ for the first desired trajectory

Ctr/ave.am	u_1	u_2	u_3	u_4	u_5	u_6
Ctr 2	65.88	30.90	6.31	0.0048	0.0049	3.85
Ctr 2+	19.01	7.9	2.79	0.0046	0.0047	3.84

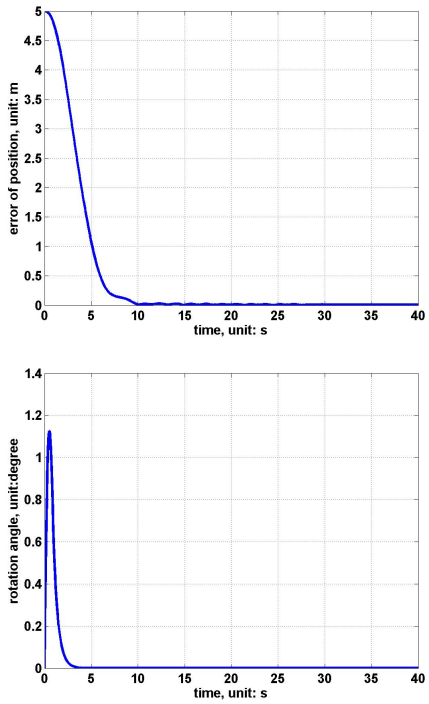

Fig. 6. The simulated generalized position error and rotation angle for the second desired trajectory during $0 \sim 40s$: Controller 2+

5.3.2 *The second desired trajectory*

Controller 2+ based on the proposed hierarchical control scheme can stabilize the simulated vehicle, as shown in Fig. 6. Like the Controller 1, the Euler-angle based Controller 2 cannot stabilize the simulated vehicle under this condition.

5.4 *Summary of the simulation results*

The dynamic model of the ODIN vehicle and two trajectories were used to test the performances of the controllers. We compared the performances between Controller 1 and Controller 1+, and the performances between Controller 2 and Controller 2+. The aim was to clearly show the characteristics of the proposed hierarchical control scheme.

From the simulation results of the first trajectory, as compared with the original controllers Controller 1 and Controller 2, our proposed controllers show better orientation tracking performance and similar position tracking performance, and generate much smaller control input signals during the starting stage. This phenomenon is not strange because Controller 1 and Controller 2 employ the Euler-angle as the orientation representation and their control input signals make $\dot{e}_p \to -\sigma e_p$ where $e_p = p - p_d$. In our proposed hierarchical control scheme, the virtual angular velocity ω_r is designed for the rotation angle $\Delta\theta$ and the virtual linear velocity v_r makes $\dot{e}_p \to -\sigma \frac{e_p}{\|e_p\|}(1 - e^{-\|e_p\|})$ such that the amplitudes of the control input signals are much less than

that of the original controllers when $\|e_p\|$ is large, e.g., during the starting stage.

Without additional supplemental techniques, the Euler-angle based Controller 1 and Controller 2 cannot be used to track the trajectory in which the pitch angle is not always far away from $\pm 90^\circ$. However, there is no singularity problem for the proposed Controller 1+ and Controller 2+.

6 Conclusion and Future Work

In this paper, a hierarchical control scheme consisting of the kinematic level and the dynamic level for fully actuated AUVs was proposed. On the kinematic level, the virtual velocity is designed. The vehicle will track the desired trajectory if the vehicle's velocity converges to the virtual velocity. On the dynamic level, two model-free controllers were developed with stability analysis.

Numerical simulations using ODIN vehicle model validated our proposed method. For the first desired trajectory, in which the desired orientation is always far away from the singularity in terms of Euler-angle, the proposed controllers achieve better performance in the rotation tracking, similar performance in the position tracking, as compared with the original controllers. The control input signals by the proposed controllers are much smaller than those by the original controllers during the starting stage. For the second trajectory, in which sometimes the desired orientation is close to singularity in terms of Euler-angle, the proposed controllers can stabilize the vehicle while the original controllers can not stabilize the vehicle.

The advantages of the proposed scheme can be concluded as:

- The hierarchical design simplifies the complexity of the trajectory tracking problem.
- Many existing methods for the control of uncertain nonlinear systems can be used in the scheme.
- The bounded and smooth design of the virtual velocity is shown to be helpful to reduce the amplitude of the control input.
- The orientation singularity is avoided.

Future work includes two aspects. Firstly, it is desirable to develop a model-based controller as a feedforward term coupled with the proposed model-free controllers so as to reduce the model uncertainty and improve the performance. Secondly, a more advanced RISE type controller taken into account the input saturation is planned to be developed.

References

[1] M. Santhakumar and T. Asokan, "Coupled, non-linear control system design for autonomous underwater vehicle (auv)," in *Control, Automation, Robotics and Vision, 2008. ICARCV 2008. 10th International Conference on*, Dec 2008, pp. 2309–2313.

[2] M. Breivik and T. Fossen, "A unified control concept for autonomous underwater vehicles," in *American Control Conference, 2006*, June 2006, pp. 7 – 13.

[3] P. W. Van De Ven, T. A. Johansen, A. J. Sørensen, C. Flanagan, and D. Toal, "Neural network augmented identification of underwater vehicle models," *Control Engineering Practice*, vol. 15, no. 6, pp. 715–725, 2007.

[4] A. Tiano, R. Sutton, A. Lozowicki, and W. Naeem, "Observer kalman filter identification of an autonomous underwater vehicle," *Control Engineering Practice*, vol. 15, no. 6, pp. 727–739, 2007.

[5] D. A. Smallwood and L. L. Whitcomb, "Preliminary experiments in the adaptive identification of dynamically positioned underwater robotic vehicles," in *Intelligent Robots and Systems, 2001. Proceedings. 2001 IEEE/RSJ International Conference on*, vol. 4. IEEE, 2001, pp. 1803–1810.

[6] P. Ridao, A. Tiano, A. El-Fakdi, M. Carreras, and A. Zirilli, "On the identification of non-linear models of unmanned underwater vehicles," *Control Engineering Practice*, vol. 12, no. 12, pp. 1483–1499, 2004.

[7] N. Miskovic, Z. Vukic, and M. Barisic, "Identification of coupled mathematical models for underwater vehicles," in *OCEANS 2007-Europe*. IEEE, 2007, pp. 1–6.

[8] M. Hosny, M. Amr, I. Zedan, M. AbdelSalam, and M. Al-Sayd, "Computational fluid dynamics-based system identification of marine vehicles," in *Computing, Communication and Networking Technologies (ICCCNT), 2014 International Conference on*, July 2014, pp. 1–7.

[9] R. Yang, B. Clement, A. Mansour, M. Li, and N. Wu, "Modeling of a complex-shaped underwater vehicle for robust control scheme," *Journal of Intelligent & Robotic Systems*, pp. 1–16, 2015.

[10] K. S. Narendra and A. M. Annaswamy, *Stable Adaptive Systems*. Courier Corporation, 2012.

[11] T. I. Fossen, *Guidance and Control of Ocean Vehicles*. Chichester; New York: Wiley, 1994.

[12] G. Antonelli, F. Caccavale, S. Chiaverini, and L. Villani, "Tracking control for underwater vehicle-manipulator systems with velocity estimation," *Oceanic Engineering, IEEE Journal of*, vol. 25, no. 3, pp. 399–413, 2000.

[13] G. Antonelli, F. Caccavale, S. Chiaverini, and G. Fusco, "A novel adaptive control law for underwater vehicles," *Control Systems Technology, IEEE Transactions on*, vol. 11, no. 2, pp. 221–232, 2003.

[14] D. A. Smallwood and L. L. Whitcomb, "Model-based dynamic positioning of underwater robotic vehicles: theory and experiment," *Oceanic Engineering, IEEE Journal of*, vol. 29, no. 1, pp. 169–186, 2004.

[15] C. McFarland and L. Whitcomb, "Experimental evaluation of adaptive model-based control for underwater vehicles in the presence of unmodeled actuator dynamics," in *Robotics and Automation (ICRA), 2014 IEEE International Conference on*, May 2014, pp. 2893–2900.

[16] D. Yoerger and J.-J. Slotine, "Adaptive sliding control of an experimental underwater vehicle," in *Robotics and Automation, 1991. Proceedings., 1991 IEEE International Conference on*, Apr 1991, pp. 2746–2751 vol.3.

[17] J. H. Kim, K. R. Lee, Y. C. Cho, H. H. Lee, and H. B. Park, "Mixed h_2 and h_∞ control with regional pole placements for underwater vehicle systems," in *American Control Conference, 2000. Proceedings of the 2000*, vol. 1, no. 6, Sep 2000, pp. 80–84 vol.1.

[18] C. E. Rohrs, L. Valavani, M. Athans, and G. Stein, "Robustness of continuous-time adaptive control algorithms in the presence of unmodeled dynamics," *Automatic Control, IEEE Transactions on*, vol. 30, no. 9, pp. 881–889, 1985.

[19] J. Yuh, "Learning control for underwater robotic vehicles," *Control Systems, IEEE*, vol. 14, no. 2, pp. 39–46, 1994.

[20] L.-J. Zhang, X. Qi, and Y.-J. Pang, "Adaptive output feedback control based on drfnn for auv," *Ocean Engineering*, vol. 36, no. 9, pp. 716–722, 2009.

[21] E. Sebastián and M. A. Sotelo, "Adaptive fuzzy sliding mode controller for the kinematic variables of an underwater vehicle," *Journal of Intelligent and Robotic Systems*, vol. 49, no. 2, pp. 189–215, 2007.

[22] J. Yuh, J. Nie, and C. Lee, "Experimental study on adaptive control of underwater robots," in *Robotics and Automation, 1999. Proceedings. 1999 IEEE International Conference on*, vol. 1, 1999, pp. 393–398 vol.1.

[23] S. Zhao and J. Yuh, "Experimental study on advanced underwater robot control," *Robotics, IEEE Transactions on*, vol. 21, no. 4, pp. 695–703, 2005.

[24] B. Xian, D. M. Dawson, M. S. de Queiroz, and J. Chen, "A continuous asymptotic tracking control strategy for uncertain multi-input nonlinear systems," in *Intelligent Control. 2003 IEEE International Symposium on*. IEEE, 2003, pp. 52–57.

[25] N. Fischer, S. Bhasin, and W. Dixon, "Nonlinear control of an autonomous underwater vehicle: A rise-based approach," in *American Control Conference (ACC), 2011*. IEEE, 2011, pp. 3972–3977.

[26] R. M. Murray, Z. Li, S. S. Sastry, and S. S. Sastry, *A Mathematical Introduction To Robotic Manipulation*. CRC press, 1994.

[27] N. Fischer, D. Hughes, P. Walters, E. M. Schwartz, and W. E. Dixon, "Nonlinear rise-based control of an autonomous underwater vehicle," *Robotics, IEEE Transactions on*, vol. 30, no. 4, pp. 845–852, 2014.

[28] T. I. Fossen, *Handbook Of Marine Craft Hydrodynamics And Motion Control*. John Wiley & Sons, 2011.

[29] S. K. Choi and J. Yuh, "Experimental study on a learning control system with bound estimation for underwater robots," *Autonomous Robots*, vol. 3, no. 2-3, pp. 187–194, 1996.

[30] B. Bidikli, E. Tatlicioglu, A. Bayrak, and E. Zergeroglu, "A new robust integral of sign of error feedback controller with adaptive compensation gain," in *Decision and Control (CDC), 2013 IEEE 52nd Annual Conference on*. IEEE, 2013, pp. 3782–3787.

[31] H. K. Khalil and J. Grizzle, *Nonlinear Systems*. Prentice hall New Jersey, 1996, vol. 3.

[32] J. Nie, J. Yuh, E. Kardash, and T. I. Fossen, "On-board sensor-based adaptive control of small uuvs in very shallow water," *International Journal of Adaptive Control and Signal Processing*, vol. 14, no. 4, pp. 441–452, 2000.

[33] T. K. Podder, G. Antonelli, and N. Sarkar, "Fault tolerant control of an autonomous underwater vehicle under thruster redundancy: Simulations and experiments," in *Robotics and Automation, 2000. Proceedings. ICRA'00. IEEE International Conference on*, vol. 2. IEEE, 2000, pp. 1251–1256.

A Figures for some control inputs

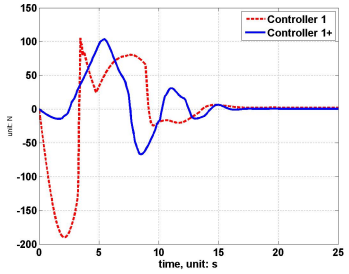

Fig. A.1. The control input u_1 for first trajectory: Controller 1 and Controller 1+

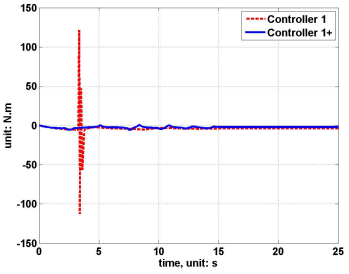

Fig. A.2. The control input u_6 for first trajectory: Controller 1 and Controller 1+

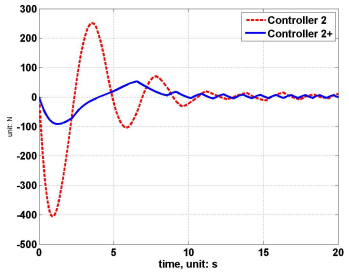

Fig. A.3. The control input u_1 for the first trajectory: Controller 2 and Controller 2+

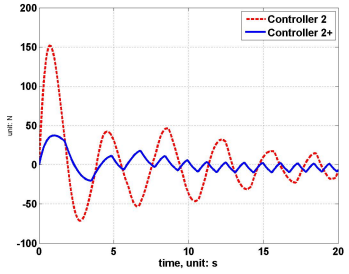

Fig. A.4. The control input u_2 for the first trajectory: Controller 2 and Controller 2+